Theoretical investigation of graphene monolayer in the presence of Fe dopant and vacancy

Md Surov Rahman

Report submitted to the Department of Physics at
Jashore University of Science and Technology
in partial fulfillment of the requirements
for the degree of Bachelor of Science
with Honours in Physics

January 2022

Abstract

The effects of Fe doping and vacancies on the electrical, magnetic, and optical characteristics of graphene are investigated using density functional theory calculations in this paper. The electronic density of states is used to reveal the conductive behavior of various defective graphene. Defected structures, on the other hand, have different magnetic and optical properties than pure structures. The static dielectric constant rises dramatically in the presence of a defect and under parallel polarization of light, and the greatest peak of Imaginary dielectric shifts red in comparison to pure graphene.Furthermore, under the same conditions, the greatest absorption peak broadens in the visible to infrared region, and the amplitude and related energy of peaks shift to higher values in the EELS spectra. Furthermore, the results demonstrate that the red and blue shifts are represented by the maximum values of refractive index and reflectivity spectra, which grow fast. In general, substituting Fe for C has a greater impact on magnetic and optical properties than C vacancies.

Acknowledgements

I would like to acknowledge and give my warmest thanks to my supervisor Dr. Mohammad Abdur Rashid who made this work possible. His guidance and advice carried me through all the stages of writing my project. I would also like to thank my group members for letting my defense be an enjoyable moment, and for your brilliant comments and suggestions, thanks to you. I would also like to give special thanks to my family as a whole for their continuous support and understanding when undertaking my research and writing my project. Your prayer for me was what sustained me this far.
Finally, I would like to praise and thank almighty Allah, for letting me through all the difficulties. I have experienced your guidance day by day. You are the one who let me finish my degree. I will keep on trusting you for my future.

Contents

List of Figures

List of Tables

Theoretical investigation of graphene monolayer in the presence of Fe dopant and vacancy

Chapter 1

Introduction

In modern time, the new sector in electronics is spintronics which also known as spin electronics. Transmitting more data with the less energy dealings is the main purpose of spintronics. High transparency, extremely high mobility, zero dark current when used as photosensitive devices and spin relaxation length more than 1.5 μm are the amazing properties of graphene. So, now the researchers are doing more researches on graphene. Hence, at the first search, graphene is a competent element for use in optoelectronic applications kind of optical gas sensor, solar cells, LEDs, photodetectors. Nevertheless, pure graphene has no magnetic properties. So, it is not suitable for spintronics. Consequently, accumulation of magnetic layer on the graphene surface, creating defect in the crystal structure of graphene such as vacancies and exchanging carbon atoms with the d-type transition metals are the better option to overcome this problem. The low concentration of defects is a proper process that also remains the metallic behaviour of graphene. Actually, the difference between spin-up and spin-down band gap energy of transitional metal (Fe, Co and Ni) doped graphene enhances its application in spintronic field. Moreover, the addition of Fe on graphene layer with a low cost and environmental friendly behaviour can act as a pos-

sible pt-free alternative catalyst for fuel cells and highly stable absorbent. Researchers have previously shown that Nitrogen oxides and H_2CO gas sensors can be made with Fe doped graphene.

Now, computers are an integral part in the world of science. It is used for calculatory problems. When problems cannot be solved analytically, computers and numerical methods are of diametrical importance. The field of computational chemistry discuss about the calculatory determination of energies, charge distribution, di- and multipoles as well as spectroscopic quantities of molecules. Get inside into molecular processes observed in research as well as in order to compute them is it's goal. The fields of molecular physics and solid state physics is associated with the determination of molecular and atomic properties.

The first steps to deal with the complex and analytically not accessible many-body Schrödinger equation were achieved by Hartree and Fock, who derived a set of self-consistant, wave function based equations which allowed an iterative calculation of energies and other desired parameters [1]. We use the Hartree-Fock method in nuclear physics and theoretical chemistry. The mathod has its faults which will be discussed in this thesis. One of major problems is high cost of computation time when large systems are executed, which arises, among other things, from the dependency of the many-body wave function on $3N$ spatial variables.

The use of less complex base variables may be a method for lower computational cost of molecular calculations. Hohenberg and Kohn provided the basis for a method in 1964. This method for the calculation of the electronic energy is rooted in DFT, which has allowed a certain improvement in the computing probability of dynamics estimation in polymers and other chemical systems. Actually, the spatial variables with the use of the DFT are reduced from $3N$ to 3, with N corresponding to the number of electrons

in the system under exploration. On the basis of the Thomas-Fermi model, DFT was first developted in the early 20th century and later formalized by the Hohenberg-Kohn theorems [2]. In 1965 Kohn and Sham derived a set of self-consistent, iteratively solvable equations which finally allowed to use the up to that point only theoretical concept of Hohenberg and Kohn also in actual computer simulations and this theory has established the foundation for the use of DFT in computational chemistry [3]. At the principle of this theory, ground state properties of a system can be completely determined by electron density. Since electron density is a much less complex quantity than the wave function, the computation times of DFT calculations are significantly lower.

Nowadays, DFT is used to calculate the atomic structure, band structure, density of state and other molecular properties of a many-body system. The purpose of DFT is to design functionals which relate electron energy to electron density function.

Chapter 2

Basic Quantum Mechanics

2.1 Schrödingers groundbreaking equation

In 1926, Erwin Schrödinger's attempt to describe the so-called 'matter waves', where he expressed de Broglie's hypothesis concerning the wave behaviour of matter in a mathematical form to describe hypothetical plane waves, which is called the time-dependent Schrödinger equation [4].

$$i\hbar\frac{\partial}{\partial t}\Psi(\vec{r},t) = \hat{H}\Psi(\vec{r},t) \tag{2.1}$$

Here, i is the square root of -1. And the function Ψ varies with time and position. Since a complete relativistic formulation of a formula is not practicable, Schrödinger himself postulated a non-relativistic approximation which is used especially in quantum chemistry.

The Hamiltonian for a single particle is taken to be

$$\hat{H} = \hat{T} + \hat{V} = -\frac{\hbar^2}{2m}\vec{\nabla}^2 + V(\vec{r},t) \tag{2.2}$$

The (non-relativistic) time-dependent single-particle Schrödinger equation becomes,

$$i\hbar\frac{\partial}{\partial t}\Psi(\vec{r},t) = \left[-\frac{\hbar^2}{2m}\vec{\nabla}^2 + V(\vec{r},t)\right]\Psi(\vec{r},t) \tag{2.3}$$

Again, using the Hamiltonian for N particles in 3D space,

$$\hat{H} = \sum_{i=1}^{N}\frac{\hat{p_i}^2}{2m_i} + V(\vec{r}_1,\vec{r}_2,\ldots,\vec{r}_N,t) = -\frac{\hbar^2}{2}\sum_{i=1}^{N}\frac{1}{m_i} + V(\vec{r}_1,\vec{r}_2,\ldots,\vec{r}_N,t) \tag{2.4}$$

The corresponding Schrödinger equation can be written as,

$$i\hbar\frac{\partial}{\partial t}\Psi(\vec{r}_1,\vec{r}_2,\ldots,\vec{r}_N,t) = \left[-\frac{\hbar^2}{2}\sum_{i=1}^{N}\frac{1}{m_i}\nabla_i^2 + V(\vec{r}_1,\vec{r}_2,\ldots,\vec{r}_N,t)\right]\Psi(\vec{r}_1,\vec{r}_2,\ldots,\vec{r}_N,t) \tag{2.5}$$

2.2 Time-independent equation

In quantum mechanics, out of all operators, the Hamiltonian (energy operator) plays an important role because it describes how the system evolves over time through Schrödinger equation. Here, this Schrödinger equation indicates the time-independent potential $V(\vec{r}_1,\vec{r}_2,\ldots,\vec{r}_N)$. And the solution of this equation represents standing waves which are called stationary states.

The time-dependent Schrödinger equation for N particles is

$$E\Psi(\vec{r}_1,\vec{r}_2,\ldots,\vec{r}_N,t) = \hat{H}\Psi(\vec{r}_1,\vec{r}_2,\ldots,\vec{r}_N,t) \tag{2.6}$$

Using the method of separation of variables for separating the spatial and the temporal part of the wave function to obtain the time-independent Schrödinger equation [5],

$$\Psi(\vec{r}_1,\vec{r}_2,\ldots,\vec{r}_N,t) = \psi(\vec{r}_1,\vec{r}_2,\ldots,\vec{r}_N)\tau(t) = \psi(\vec{r}_1,\vec{r}_2,\ldots,\vec{r}_N)\cdot e^{-i\omega t} \tag{2.7}$$

The general eigenvalue equation of time-independent Schrödinger equation can be written as,

$$E\psi(\vec{r}_1, \vec{r}_2, \ldots, \vec{r}_N) = \hat{H}\psi(\vec{r}_1, \vec{r}_2, \ldots, \vec{r}_N) \tag{2.8}$$

The corresponding Schrödinger equation for many-body Hamiltonian becomes,

$$E\psi(\vec{r}_1, \vec{r}_2, \ldots, \vec{r}_N) = \left[-\frac{\hbar^2}{2} \sum_{i=1}^{N} \frac{1}{m_i} \nabla_i^2 + V(\vec{r}_1, \vec{r}_2, \ldots, \vec{r}_N) \right] \psi(\vec{r}_1, \vec{r}_2, \ldots, \vec{r}_N) \tag{2.9}$$

2.3 The wave function

Material particles possess wave-like properties and electromagnetic radiation shows particle-like behavior, which is called wave-particle duality. The first and vital postulate of quantum mechanics is that the state of a particle is completely described by its wave function (time-dependent), which contains all essential information about the particle's state.

On account of simplicity, the discussion is confined to the time-independent wave function. The wave function is represented by Ψ in quantum mechanics, which has no physical interpretation. In 1926, Max Born published a probability interpretation of the wave function, which is a major principle of the Copenhagen interpretation of quantum mechanics, provides a physical interpretation for the square of the absolute quantity of the wave function as a probability density [6].

$$|\psi(\vec{r}_1, \vec{r}_2, \ldots, \vec{r}_N)|^2 d\vec{r}_1 d\vec{r}_2 \ldots d\vec{r}_N \tag{2.10}$$

The particles $1, 2, \ldots, N$ are lying simultaneously in the corresponding volume element $d\vec{r}_1 d\vec{r}_2 \ldots d\vec{r}_N$ which is the probability that is described by equation (2.10) [7]. If the positions of two particles are exchanged, the

overall probability density cannot depend on such an exchange. That is,

$$|\psi(\vec{r}_1, \vec{r}_2, \ldots, \vec{r}_i, \vec{r}_j, \ldots, \vec{r}_N)|^2 = |\psi(\vec{r}_1, \vec{r}_2, \ldots, \vec{r}_j, \vec{r}_i, \ldots, \vec{r}_N)|^2 \qquad (2.11)$$

The symmetrical and anti-symmetrical wave functions are two possibilities for the behavior of the wave function during a particle exchange. The symmetrical wave function does not change due to such an exchange, which corresponds bosons (integer or zero spin). But the anti-symmetrical wave function change itself sign that corresponds fermions (half-integer spin) [8]. Since electrons are fermions, the anti-symmetric fermion wave function can be discussed in this thesis. The anti-symmetric fermion wave function follows the Pauli exclusion principle, which states that no two electrons can occupy the same orbital.

Normalization of a wave function is another outcome of the probability interpretation. Wave function of a particle must be normalized. The probability of finding the particle somewhere in space is unity, which is normalization condition for the wave function.

$$\int d\vec{r}_1 \int d\vec{r}_2 \ldots \int d\vec{r}_N |\psi(\vec{r}_1, \vec{r}_2, \ldots, \vec{r}_N)|^2 = 1 \qquad (2.12)$$

Equation (2.12) has physical acceptance. Wave function must be continuous and square-integrable. Any wave function which is not continuous and square-integrable has no physical meaning in quantum mechanics [9].

Calculating the expectation values of operators with a wave function provides the expectation value of the corresponding observable for that wave function, which is another essential property of the wave function [10]. For an observable $A(\vec{r}_1, \vec{r}_2, ..., \vec{r}_N)$, this can be written as,

$$A = \langle A \rangle = \int d\vec{r}_1 d\vec{r}_2 \ldots \int d\vec{r}_N \psi^*(\vec{r}_1, \vec{r}_2, \ldots, \vec{r}_N) \hat{A} \psi(\vec{r}_1, \vec{r}_2, \ldots, \vec{r}_N) \quad (2.13)$$

2.4 Atoms and Molecules

The single electron time-independent Schrödinger equation reads,

$$i\hbar\frac{\partial}{\partial t}\psi(\vec{r}) = \left[-\frac{\hbar^2}{2m}\vec{\nabla}^2 - \frac{e^2}{4\pi\epsilon_0}\cdot\frac{1}{|\vec{r}|}\right]\psi(\vec{r}) \tag{2.14}$$

Here, the electron mass m_e, the elementary charge e, the reduced plank constant (Dirac constant) $\hbar$, and the vacuum permittivity fator $4\pi\epsilon_0$ [11]. The Schrödinger equation is simplified to,

$$E\psi(\vec{r}) = \left[-\frac{1}{2}\vec{\nabla}^2 - \frac{1}{|\vec{r}|}\right]\psi(\vec{r}) \tag{2.15}$$

This type of Schrödinger equation is analytically solvable.
Again, the Schrödinger equation can be written as,

$$E_i\psi_i(\vec{r}_1,\vec{r}_2,\ldots,\vec{r}_N,\vec{R}_1,\vec{R}_2,\ldots,\vec{R}_M) = \hat{H}\psi(\vec{r}_1,\vec{r}_2,\ldots,\vec{r}_N,\vec{R}_1,\vec{R}_2,\ldots,\vec{R}_M) \tag{2.16}$$

Where, Hamilton operator $\hat{H}$ for a system composed of M nuclei and N electrons in the absence of external magnetic and electric field.
The Hamiltonian corresponds to,

$$\hat{H} = -\frac{1}{2}\sum_{i=1}^{N}\nabla_i^2 - \frac{1}{2}\sum_{k=1}^{M}\nabla_k^2 - \sum_{i=1}^{N}\sum_{k=1}^{M}\frac{Z_k}{r_{ik}} + \sum_{i=1}^{N}\sum_{j>1}^{N}\frac{1}{r_{ij}} + \sum_{k=1}^{M}\sum_{l>k}^{M}\frac{Z_kZ_l}{R_{kl}} \tag{2.17}$$

In equation (2.17), the nuclear mass is denoted by M_k in atomic unit, the atomic numbers are denoted by Z_k and Z_l and $r_{ij} = |\vec{r_i} - \vec{r_j}|$, $r_{ik} = |\vec{r_i} - \vec{R_k}|$ and $R_{kl} = |\vec{R_k} - \vec{R_l}|$ describe the distances between the particles.

The first two term in equation (2.17) expresses the kinetic energy of electron and nuclei. The sequential three terms define the potential part of the Hamiltonian and express the attractive electrostatic interaction between the nuclei and the electrons and the repulsive potential due to the electron-electron and nucleus-nucleus interaction, respectively [12].

According to the Born-Oppenheimer approximation, the core movement has no influence on electronic transitions. From equation (2.17) the so-called electronic Hamiltonian gives,

$$\hat{H_{el}} = -\frac{1}{2}\sum_{i=1}^{N}\nabla_i^2 - \sum_{i=1}^{N}\sum_{k=1}^{M}\frac{Z_k}{r_{ik}} + \sum_{i=1}^{N}\sum_{j>1}^{N}\frac{1}{r_{ij}} \tag{2.18}$$

$$= \hat{T} + \hat{U} + \hat{V} \tag{2.19}$$

$$= \hat{T} + \hat{V}_{tot} \tag{2.20}$$

In equation (2.19), the kinetic energy term $\hat{T}$ and the electron-electron repulsion $\hat{U}$ do not depend on the nuclear coordinates R_{kl}. And the external potential $\hat{V}$ depends on the atomic system caused by the nucleus-electron repulsion, where are no external magnetic or electric fields [10]. $\hat{T}$ and $\hat{V}$ only depend on the electron number N. The external potential is the next step to determination of the wave functions.

2.5 The variational principle

If we can't find a solution to the Schrödinger equation analytically, a recipe known as the variational principle that is a specialized approach that may be used to calculate the ground-state energy of a system. It is similar to the least-action principle of classical mechanics because of corresponding to the lowest energy of the system.

From the interest of the electric Schrödinger equation, we can set, $\hat{H} \equiv \hat{H}_{el}$, $E \equiv E_{el}$. The expectation value of a particular observable represented by the appropriate operator $\hat{A}$ using any trial normalized wave function ψ_{trial}

can be written as,

$$\langle \hat{A} \rangle = \int d\vec{r}_1 \int d\vec{r}_2 \ldots \int d\vec{r}_N \psi^*_{trial}(\vec{r}_1, \vec{r}_2, \ldots, \vec{r}_N) \hat{A} \psi_{trial}(\vec{r}_1, \vec{r}_2, \ldots, \vec{r}_N) \tag{2.21}$$

$$\equiv \langle \psi_{trial} | \hat{A} | \psi_{trial} \rangle \tag{2.22}$$

where, the bra-ket notation of Dirac is introduced and ψ^*_{trial} indicates the complex conjugate of ψ_{trial}.

Using the trial wave function (normalized), the energy as observable are calculated as the expectation values of Hamilton operator, i.e.,

$$E_{trial} = \int d\vec{r}_1 \int d\vec{r}_2 \ldots \int d\vec{r}_N \psi^*_{trial}(\vec{r}_1, \vec{r}_2, \ldots, \vec{r}_N) \hat{H} \psi_{trial}(\vec{r}_1, \vec{r}_2, \ldots, \vec{r}_N) \tag{2.23}$$

For ground-state energy,

$$E_0 = \int d\vec{r}_1 \int d\vec{r}_2 \ldots \int d\vec{r}_N \psi^*_0(\vec{r}_1, \vec{r}_2, \ldots, \vec{r}_N) \hat{H} \psi_0(\vec{r}_1, \vec{r}_2, \ldots, \vec{r}_N) \tag{2.24}$$

The variational principle now states that the energy obtained by this trial wave function will be an upper bound to the true energy of the ground state [13]. If ψ_{trial} and ψ_0 are uniform, the equality will be maintained. i.e.,

$$\langle \psi_{trial} | \hat{H} | \psi_{trial} \rangle = E_{trial} \geq E_0 = \langle \psi_0 | \hat{H} | \psi_0 \rangle \tag{2.25}$$

Proof [13]: Since the eigenfunction ψ_i of the Hamiltonian $\hat{H}$ from a complete set, we can express the normalized trial wave function ψ_{trial} as a linear combination of them.

$$\psi_{trial} = \sum_i \lambda_i \psi_i \tag{2.26}$$

Since ψ_{trial} is normalized,

$$\langle \psi_{trial} | \psi_{trial} \rangle = 1 = \langle \sum_i \lambda_i \psi_i | \sum_j \lambda_j \psi_j \rangle = \sum_i \sum_j \lambda^*_i \lambda_j \langle \psi_i | \psi_j \rangle = \sum_j |\lambda_j|^2 \tag{2.27}$$

Assume that, the eigenfunctions are orthogonal and normalized. From equation (2.25) and (2.27),

$$E_{trial} = \langle \psi_{trial} | \hat{H} | \psi_{trial} \rangle = \langle \sum_i \lambda_i \psi_i | \hat{H} | \sum_j \lambda_j \psi_j \rangle = \sum_j E_j |\lambda_j|^2 \qquad (2.28)$$

By the defination, the ground-state energy is the lowest eigenvalue ($E_0 \leq E_i$), it follows that

$$E_{trial} = \sum_j E_j |\lambda_j|^2 \geq E_0 \sum_j |\lambda_j|^2 \qquad (2.29)$$

The main mathematical concept of density functional theory is used above, which assigns a numerical number (E_{trial}) to a function (ψ_{trial}) is called functional. For finding the ground state energy and wave function, the functional $E[\psi_{trial}]$ have to minimize by searching through all allowed N-electron wave functions. Allowed wave function means this following wave function must be continuous everywhere and be quadratic integrable. The ground state energy can be written as,

$$E_0 = \min_{\psi \to N} E[\psi] = \min_{\psi \to N} \langle \psi | \hat{H} | \psi \rangle = \min_{\psi \to N} \langle \psi | \hat{T} + \hat{V} + \hat{U} | \psi \rangle \qquad (2.30)$$

where, $\psi \to N$ represents all allowed N-electron wave function. The search over all allowed N-electron wave function is apparently not possible due to the large amount of possible wave function and huge calculation time. The variational principle can be applied to subsets of all possible wave function, which is done in the Hartree-Fock approximation.

2.6 The Hartree-Fock Approximation

In 1948, Hartree published an approximation method for finding the best possible one-electron wave functions and two years later this method is developed by Fock. From above discussion, equation (2.30) can not be solved by searching all allowed N-electron wave function. So, define a suitable sub-

set is needed for it. In the Hartree-Fock process, physically good approximation to the complex many electron wave function is improved. It consists of approximating the N-electron wave function by an anti-symmetric product of N one-electron wave function, which is called spin-orbitals $\chi_i(\vec{x}_i)$ [14]. This product of this type is called Slater-determinant ϕ_{SD} that specifies to

$$\psi_0 \approx \phi_{SD} = (N!)^{-\frac{1}{2}} \begin{bmatrix} \chi_1(\vec{x}_1) & \chi_2(\vec{x}_1) & \dots & \chi_N(\vec{x}_1) \\ \chi_1(\vec{x}_2) & \chi_2(\vec{x}_2) & \dots & \chi_N(\vec{x}_2) \\ \vdots & \vdots & \ddots & \vdots \\ \chi_1(\vec{x}_N) & \chi_2(\vec{x}_N) & \dots & \chi_N(\vec{x}_N) \end{bmatrix} \tag{2.31}$$

Using a suitable short-hand notation, it can be written as

$$\phi_{SD} = \frac{1}{\sqrt{N!}} \det\{\chi_1(\vec{x}_1) \quad \chi_2(\vec{x}_2) \dots \chi_N(\vec{x}_N)\} \tag{2.32}$$

where, $(N!)^{-\frac{1}{2}}$ represents a normalization factor. In this slater determinant, N electrons hold N spin orbitals $(\chi_1, \chi_2, \dots, \chi_N)$ without specifying which electron is in which orbital.

The spin orbitals are composed of a spatial orbital $\phi_i(\vec{r})$ and the spatial parts of the spin orbitals have two spin functions that is $\alpha(s)$ and $\beta(s)$.

$$\chi(\vec{x}) = \phi(\vec{r})\sigma(s) \tag{2.33}$$

where, $\sigma = \alpha, \beta$. The essential property of the spin functions is that they are orthonormal, that is $\langle\alpha|\alpha\rangle = \langle\beta|\beta\rangle = 1$ and $\langle\alpha|\beta\rangle = \langle\beta|\alpha\rangle = 0$. Two spin functions satisfy the relation, i.e.

$$\int \chi_i^*(\vec{x})\chi_j(\vec{x})dx = \langle\chi_i|\chi_j\rangle = \delta_{ij} \tag{2.34}$$

Here, δ_{ij} represents Kronecker delta which is equal to 1 for $i = j$ and 0 for otherwise. Spin orbitals convey the usual physical interpretation that $|\chi(\vec{x})|^2 d\vec{x}$ indicates the probability of finding the electron with spin given by σ within the volume element $d\vec{r}$.

Now, the variational principle is applied due to find the best Slater determinant, i.e.

$$E_0 = \min_{\phi_{SD}\to N} E[\phi_{SD}] = \min_{\phi_{SD}\to N} \langle\phi_{SD}|\hat{H}|\phi_{SD}\rangle = \min_{\phi_{SD}\to N} \langle\phi_{SD}|\hat{T}+\hat{V}+\hat{U}|\phi_{SD}\rangle \tag{2.35}$$

Using the slater determinant, the Hartree-Fock energy is simplified to

$$E_{HF} = \langle\phi_{SD}|\hat{H}|\phi_{SD}\rangle = \langle\phi_{SD}|\hat{T}+\hat{V}+\hat{U}|\phi_{SD}\rangle \tag{2.36}$$

On account of simplicity, an elaborated derivation of the final expression for the Hartree-Fock energy is eliminated. The final expression for the Hartree-Fock energy can be written as

$$E_{HF} = \langle\phi_{SD}|\hat{H}|\phi_{SD}\rangle = \sum_{i}^{N}(i|\hat{h}|i) + \frac{1}{2}\sum_{i}^{N}\sum_{j}^{N}[(ii|jj) - (ij|ji)] \tag{2.37}$$

where,

$$(i|\hat{h}|i) = \int \chi_i^*(\vec{x}_i)\left[-\frac{1}{2}\vec{\nabla}_i^2 - \sum_{k=1}^{M}\frac{Z_k}{r_{ik}}\right]\chi_i(\vec{x}_i)d\vec{x}_i \tag{2.38}$$

$$(ii|jj) = \iint |\chi_i(\vec{x}_i)|^2\frac{1}{r_{ij}}|\chi_j(\vec{x}_j)|^2 d\vec{x}_i d\vec{x}_j \tag{2.39}$$

$$(ij|ji) = \iint \chi_i(\vec{x}_i)\chi_j^*(\vec{x}_i)\frac{1}{r_{ij}}\chi_j(\vec{x}_j)\chi_i^*(\vec{x}_j)d\vec{x}_i d\vec{x}_j \tag{2.40}$$

The first term defines the contribution due to the kinetic energy and electron-nucleus interaction, where $\hat{h}$ indicates the single particle contribution of the Hamiltonian. And the sequential two terms become electron-electron interaction, which are called coulomb and exchange integrals, respectively.

From equation (2.37), E_{HF} is expressed as a functional of the spin orbitals, $E_{HF} = E[\chi_i]$. Thus, the variational freedom in this expression leads to the minimum energy. Moreover, the spin orbitals must be orthonormal during minimization, which expresses as the Lagrangian multipliers ϵ_i in the resulting equations. These equations are Hartree-Fock equations, which can

be written as (for a detailed derivation follow Szabo and Ostland 1982)

$$\hat{f}\chi_i = \lambda_i \chi_i \qquad\qquad i = 1, 2, \ldots, N \tag{2.41}$$

with

$$\hat{f}_i = -\frac{1}{2}\vec{\nabla}_i^2 - \sum_{k=1}^{M} \frac{Z_k}{r_{ik}} + \sum_{i}^{N} [\hat{J}_j(\vec{x}_i) - \hat{K}_j(\vec{x}_i)] \qquad = \hat{h}_i + \hat{v}_{HF}(i) \tag{2.42}$$

where, $\hat{f}_i$ indicates the Fock operator for the i-th electron. The first two terms indicate the kinetic and potential energy due to electron-nucleus attraction. The last term $\hat{V}_{HF}$ is the Hartee-Fock potential, which has two components that is the coulomb operators $\hat{J}_j$ and the exchange operators $\hat{K}_j$ with the other j electrons. The two electron repulsion operator from the original Hamiltonian is exchanged by a one-electron operator $\hat{V}_{HF}$ that represents the repulsion in average [7].

2.7 Failings of the Hartree-fock approach

An even and odd number of electrons can stay in the molecules. Compounds with an even number of electrons and double occupied spatial orbitals ϕ_i that is species with singlet state, which are called closed-shell systems. The compound is in a triplet or higher ground state in case the number of electrons is odd and all of them are lying in single occupied orbitals. These systems are called open-shell systems. Two different schemes of the Hartree-Fock method is applied to these two types of systems. The restricted Hartree-Fock (RHF) model constructed with doubly occupied orbitals which minimize the total energy. On the other hand, electrons are considered to be single in orbitals in the unrestricted HF (UHF) method. Open-shell systems are also described by a RHF scheme where only the double occupied orbitals are included which is then called a restricted open-shell HF (ROHF). But the unrestricted HF (UHF) is much more popular than ROHF [7].

In order to find an appropriate result, sometimes the unrestricted scheme is applied to the closed-shell systems. Such that, the description of the separation of H_2 that is the behaviour at large internuclear distance, where one-electron must be situated at one hydrogen atom which can not be logically calculated by the use of a system which places both electrons in the same spatial orbitals. Consequently, the selection of method is always a very important point in HF calculations.

A limiting factor is used to maintain the size of the investigated system. For H_2 system, Kohn consider a number of $M = p^5$ with $3 \leq p \leq 10$ parameters to find a proper result in the observation. Taking $N = 100$ electrons for a system, we find,

$$M = p^{3N} = 3^{300} \quad to \quad 10^{300} \approx 10^{150} \quad to \quad 10^{300} \tag{2.43}$$

In equation (2.43), at least 10^{150} dimention in a space exceeds the calculation possibilities for the minimization of the energy. So, the small number of involved electrons is used to the HF method. Therefore, exponential wall is taking the exponential factor in this limitation.

The Hartree-Fock limit is the absolute maximum accuracy which can get from a Hartree-Fock calculation. According to the variational principle, the Hartree-Fock energy (E_{HF}) is always larger than the exact ground state energy (E_0) whereas a many electron wave function can not be composed entirely by a single basis set (Slater determinant). The difference between these two energies is known as correlation energy and can be written as

$$E_{corr}^{HF} = E_0 - E_{HF} \tag{2.44}$$

The elimination of electron correlation (coulomb correlation) in the HF method is at the root of the lack of HF wavefunction in describing the real

atoms and molecules.

Chapter 3

Density functional theory

3.1 A new base variable : electron density

The wave function ψ, a general statement about the calculation of observables which contains all information has been provided in the section 2.3. A similar approach is described in this section for a quantity calculation. The electron density (for N electron) which gives probability interpretation reads [7],

$$n(\vec{r}) = N \sum_{s_1} \int d\vec{x}_2 \ldots \int d\vec{x}_N \psi^*(\vec{x}_1, \vec{x}_2, \ldots, \vec{x}_N)\psi(\vec{x}_1, \vec{x}_2, \ldots, \vec{x}_N) \quad (3.1)$$

In equation (3.1), the notation reputes a wave function dependent on spin and spatial coordinates.

It should be noted that the multiple integral represents the probability that a particular electron is found in the volume element dr_1. The probability of finding any electron at this position is N times the integral whereas electrons are indistinguishable. The wave function ψ represents the arbitrary position and spin in the state of the other $(N-1)$ electrons.

The electron density only dependent on spatial coordinates in case the spin

coordinates are neglected.

$$n(\vec{r}) = N \int d\vec{r}_2 \ldots \int d\vec{r}_N \psi^*(\vec{r}_1, \vec{r}_2, \ldots, \vec{r}_N)\psi(\vec{r}_1, \vec{r}_2, \ldots, \vec{r}_N) \tag{3.2}$$

This can be obtained by X-ray diffraction. The electron density as variable contains all essential information about the system before presenting a scheme.

The electron density integrates to the total number of electron over the spatial variables,

$$N = \int d\vec{r}_N(\vec{r}) \tag{3.3}$$

The electron density of a system of interacting electrons in some external potential determines this potential uniquely, where uniquely means up to an uninteresting additive constant.

3.2 The Hohenberg-Kohn theorems

In 1964, the Hohenberg-Kohn theorems published in the physical review (in homogeneous electron gas) that was presented by Hohenberg and Kohn [7]. The modern day density functional theories were established in this thesis. The proof runs as follows and is gained by reductio ad absurdum. This discussion deals with non-degenerate ground state, which limitation doesn't affect the presented proof for the second theorem and can later be lifted as well for the first theorem [15].
For the proof of Hohenberg and Kohn's first theorem, the energy will be used, which can be written as

$$E = \langle\psi|\hat{H}|\psi\rangle = \langle\psi|\hat{T} + \hat{V} + \hat{U}|\psi\rangle = \int v(\vec{r})n(\vec{r})d\vec{r} + \langle\psi|\hat{T} + \hat{U}|\psi\rangle \tag{3.4}$$

Theorem 1 [16]: The external potential $v(\vec{r})$ is a unique functional of the electron density $n(\vec{r})$, apart from a trivial additive constant, determined by it.

Proof [2]: It is considered that there remain two external potential $v(\vec{r})$ and $v'(\vec{r})$ which differ by more than a constant but each giving the same electron density $n(\vec{r})$ associated with the corresponding non-degenerate ground states of N particles. For different external potential, there must have to be two different Hamiltonians, $\hat{H} = \hat{T} + \hat{V}_{ee} + \hat{V}$ and $\hat{H}' = \hat{T} + \hat{V}_{ee} + \hat{V}'$. These two different Hamiltonians ground-state densities were the same although the normalized wave functions ψ and ψ' would be different. Ultimately, the ground-state energies E_0 and E_0' associated with the wave function ψ and ψ', respectively.

Taking the two trial wave functions ψ and ψ' for the $\hat{H}$ and $\hat{H}'$ problem, respectively and consider that the other wave function is the ground state wave function. This expression can be written as

$$E_0' = \langle\psi'|\hat{H}'|\psi'\rangle < \langle\psi|\hat{H}'|\psi\rangle = \langle\psi|\hat{H} + \hat{V}' - \hat{V}|\psi\rangle = \langle\psi|\hat{H}|\psi\rangle + \langle\psi|\hat{V}' - \hat{V}|\psi\rangle \tag{3.5}$$

and,

$$E_0 = \langle\psi|\hat{H}|\psi\rangle < \langle\psi'|\hat{H}|\psi'\rangle = \langle\psi'|\hat{H}' + \hat{V} - \hat{V}'|\psi'\rangle = \langle\psi'|\hat{H}'|\psi'\rangle + \langle\psi'|\hat{V} - \hat{V}'|\psi'\rangle \tag{3.6}$$

By the use of equation (3.4), equation (3.5) and (3.6) yield,

$$E_0' < E_0 + \int [v'(\vec{r}) - v(\vec{r})]n(\vec{r})d\vec{r} \tag{3.7}$$

and,

$$E_0 < E_0' + \int [v(\vec{r}) - v'(\vec{r})]n(\vec{r})d\vec{r} \tag{3.8}$$

respectively.

After adding equations (3.7) and (3.8), the inequality,

$$E_0' + E_0 < E_0 + E_0' \tag{3.9}$$

is attained.

The first Hohenberg-Kohn theorem has several alternative proof, "strong form" of the Hohenberg-Kohn theorem is one of them. Here, $\Delta v(\vec{r})$ and $\Delta n(\vec{r})$ denote the change in potential and electron density, respectively.

$$\int \Delta v(\vec{r})\Delta n(\vec{r})d\vec{r} < 0 \tag{3.10}$$

whereas equation (3.10) can be derived from the lines of the standard Hohenberg-Kohn proof, it can also be derived perturbatively.

If $\Delta v(\vec{r}) \neq 0$ clearly, we can't have $\Delta n(\vec{r}) \equiv 0$. This observation implies the first Hohenberg-Kohn theorem. The importance of this proof also provides a requirement about the sign of $\Delta n(\vec{r})$ and $\Delta v(\vec{r})$, i.e. if $\Delta v(\vec{r})$ is mostly positive, $\Delta n(\vec{r})$ must be mostly negative, in order that their integral over all space is negative. The ground state wave function is a unique functional of the ground state electron density that is obtained from the first Hohenberg-Kohn theorem.

$$\psi_0(\vec{r}_1, \vec{r}_2, \ldots, \vec{r}_N) = \psi[n_0(\vec{r})] \tag{3.11}$$

From equation (2.13), the expectation value of ground state for any observable is a functional of $n_0(\vec{r})$ too, which reads,

$$A_0 = A[n_0(\vec{r})] = \langle \psi[n_0(\vec{r})]|\hat{A}|\psi[n_0(\vec{r})]\rangle \tag{3.12}$$

The expectation value of the Hamiltonian gives the ground state energy. From equation (3.4), the ground state energy corresponding to an potential $v(\vec{r})$ can be written as

$$E_{v,0} = E_v[n_0(\vec{r})] = \langle \psi[n_0(\vec{r})|\hat{H}|\psi[n_0(\vec{r})]\rangle = \int v(\vec{r})n_0(\vec{r})d\vec{r} + \langle \psi[n_0(\vec{r})|\hat{T} + \hat{U}|\psi[n_0(\vec{r})]\rangle \tag{3.13}$$

From equation (3.13), the Hohenberg-Kohn functional $F_{HK}[n(\vec{r})]$ are obtained and then the energy functional $E_v[n(\vec{r})]$ can be denoted as

$$F_{HK}[n(\vec{r})] \equiv \langle\psi[n_0(\vec{r})]|\hat{T}+\hat{U}|\psi[n_0(\vec{r})]\rangle \tag{3.14}$$

$$E_v[n(\vec{r})] \equiv \int v(\vec{r})n_0(\vec{r})d\vec{r} + F_{HK}[n(\vec{r})] \tag{3.15}$$

where, $F_{HK}[n(\vec{r})]$ is the sum of the functional for the kinetic energy and functional for the electron-electron interaction, which represents the system independent or universal part.

Theorem 2 [16]: The ground state energy can be obtained from the electron density variationally. The electron density which minimizes the total energy, is therefore the true ground state density.

The constrained-search approach is a different way of looking at the variational search connected to the Hohenberg-Kohn second theorem which is introduced by Levy and Lieb.

A trial density $n'(\vec{r})$ defines its own trial wave function whereas a unique functional of the electron density is the wave function similar to equation. According to the variational principle, the ground state energy can be denoted as

$$E_{v,0} = \min_{\psi'}\langle\psi'|\hat{H}|\psi'\rangle \tag{3.16}$$

Proof: The minimization can be introduced in two stages in the principle. In the first stage, fix a electron density $n'(\vec{r})$ and the class of trial functions associated with the electron density can be denoted as $\psi'^{\alpha}_{n'}$. The constrained energy minimum, with $n'(\vec{r})$ fixed, is represented as

$$E_v[n'(\vec{r})] \equiv \min_{\alpha}\langle\psi'^{\alpha}_{n'}|\hat{H}|\psi'^{\alpha}_{n'}\rangle = \int v(\vec{r})n'(\vec{r})d\vec{r} + F[n'(\vec{r})] \tag{3.17}$$

where,

$$F[n'(\vec{r})] \equiv \min_{\alpha} \langle \psi_{n'}^{'\alpha} | \hat{T} + \hat{U} | \psi_{n'}^{'\alpha} \rangle \tag{3.18}$$

which is connected to the Hohenberg-Kohn functional in (3.13). The universal functional of the density $n'(\vec{r})$ is denoted as $F[n'(\vec{r})]$ which requires no explicit knowledge of $v(\vec{r})$.

In the second stage, minimize equation (3.17) over all trial densities $n'(\vec{r})$,

$$E_{v,0} = \min_{n'(\vec{r})} E_v[n'(\vec{r})] = \min_{n'(\vec{r})} \{ \int v(\vec{r}) n'(\vec{r}) d\vec{r} + F[n'(\vec{r})] \} \tag{3.19}$$

In case of a non-degenerate ground state, the minimum is attained whether $n'(\vec{r})$ is the ground state density, and for the degenerate ground state, if $n'(\vec{r})$ is any one of the ground state densities. The second stage lifts the constraint of a particular density and elaborates the search over all densities.

To summarize that the density functional theory gives a exact mathematical foundation for the use of the electron density as basis variable. In spite of that the Hohenberg-Kohn theorem can not provide any support for the calculation of molecular properties and any information about approximations for functionals like $F[n(\vec{r})]$. The variational principle used in the second theorem of Hohenberg and Kohn is more tricky than the variational principle used in Hartree-Fock method. The Hartree-Fock method is the wave function based approach but the Hohenberg-Kohn theorem is the electron density based approach. This functional gives more essential result.

The v-representability condition is stronger than the N-representability condition. The density functional theory can be composed in a strategy that only requires the density both in functionals and in variational principle to satisfy a weaker condition, the N-representability condition. At last, it is important that the possible ground state densities can fulfill the requirements, and do not correspond to a potential $v(\vec{r})$.

3.3 The self-consistent Kohn-Sham equations

The mathematical foundation by Hohenberg and Kohn is appropriate, but it is not very useful in actual calculation. The direct use of the second Hohenberg-Kohn theorem for energy minimization is the only possibility which is possible in general but has not proven itself practically. Quantities can be measured for problems without an appropriate analytical solution is the most wishful process which allows iteration.

The self-consistent single particle Hartree equations are an iterative approach which are wave function based as well as not directly related to the work of Hohenberg and Kohn, but they have been proven very useful [10]. Hartree's approximation proposes that every electron was considered as moving in as effective single particle potential,

$$v_H(\vec{r}) = -\frac{Z}{|\vec{r}|} + \int \frac{n(\vec{r}')}{|\vec{r} - \vec{r}'|} d\vec{r}' \tag{3.20}$$

where, the first term represents an attractive coulomb potential of a nucleus with atomic number Z and the potential because of the average electron density distribution $n(\vec{r})$ is the second term. Thus the single particle Schrödinger equation for each electron is

$$\left[-\frac{1}{2}\vec{\nabla}^2 + v_H(\vec{r}) \right] \phi_j(\vec{r}) = \epsilon_j \phi_j(\vec{r}) \qquad j = 1, \ldots, N \tag{3.21}$$

where, j represents both spatial and spin quantum numbers.
The mean density can be written as

$$n(\vec{r}) = \sum_{j=1}^{M} |\phi_j(\vec{r})|^2 \tag{3.22}$$

where, according to the pauli exclusion principle, the sum runs over the M lowest eigenvalues in the ground state. The self-consistent Hartree equations are defined in equation (3.20)-(3.22).

An electron density $n(\vec{r})$ and a potential $v_H(\vec{r})$ are constructed to solve these self-consistent Hartree equations iteratively that is then used to solve (3.21) for ϕ_j. The electron density $n(\vec{r})$ are recalculated from equation (3.22), which should be the similar as the initial $n(\vec{r})$. This produce iterates untill appropriate results are obtained. The task of extracting the Hartree equations from the Hohenberg-Kohn variational principle for the energy should deliver even improvements as well as further, an alternative and finally practically useful formulation of the second theorem whereas the mathematical foundation of Hohenberg and Kohn is formally appropriate. Hence, Kohn and Sham discussed the DFT similar to Hartree's approximation which has the form of the Schrödinger equation for N non-interacting electrons moving in the external potential [2].

Remembering equation (3.17) and (3.18), the expression of Hohenberg-Kohn variational principle can be written as

$$E_{v(\vec{r})}[n'(\vec{r})] \equiv \int v(\vec{r})n'(\vec{r})d\vec{r} + T_S[n'(\vec{r})] \geq E \tag{3.23}$$

where, $n'(\vec{r})$ and $T_S[n'(\vec{r})]$ denote a v-representable density for non-interacting electrons and the kinetic energy of the ground state of non-interacting electrons with density distribution $n'(\vec{r})$, respectively.
Applying the Euler-Lagrange equation for the non-interacting case (3.23) with the density $n(\vec{r})$,

$$\delta E_v[n'(\vec{r})] \equiv \int \delta n'(\vec{r}) \left[v(\vec{r}) + \frac{\delta}{\delta n'(\vec{r})} T_S[n'(\vec{r})]|_{n'(\vec{r})=n(\vec{r})} - \epsilon \right] d\vec{r} = 0 \tag{3.24}$$

Here, $n'(\vec{r})$ represents the exact ground state density for $v(\vec{r})$ and ϵ is a lagrangian multiplier to insure particle conservation.
To calculate the ground state energy and particle density of the non-interacting single particles, the approximated Hartree-potential is exchanged by a simple external potential with the help of equation (3.20) to (3.22). For this

system, the single particle Schrödinger equation can be written as

$$\{-\frac{1}{2}\vec{\nabla}^2 + v(\vec{r}) - \epsilon_j\}\phi_j(\vec{r}) = 0 \tag{3.25}$$

Giving,

$$E = \sum_{j=1}^{N} \epsilon_j \tag{3.26}$$

and

$$n(\vec{r}) = \sum_{j=1}^{N} |\phi_j(\vec{r})|^2 \tag{3.27}$$

For the problem of interacting electrons, the single-particle was addressing approximately similar as Hartree equations. Kohn and Sham used the functional $F[n'(\vec{r})]$ of equation (3.18) in the form,

$$F[n'(\vec{r})] \equiv T_S[n'(\vec{r})] + \frac{1}{2}\int \frac{[n'(\vec{r})][n'(\vec{r}')]}{|\vec{r} - \vec{r}'|} d\vec{r} d\vec{r}' + E_{xc}[n'(\vec{r})] \tag{3.28}$$

where, $T_S[n'(\vec{r})]$ denotes the kinetic energy functional for non-interacting electrons and the second term is Hartree term that describes the electrostatic self-repulsion of the electron density. The last term is the so-called exchange-correlation energy functional term which is defined by equation.

The Hohenberg-Kohn variational principle for interacting electrons can be written in the form,

$$E_{v(\vec{r})}[n'(\vec{r})] \equiv \int v(\vec{r}) n'(\vec{r}) d\vec{r} + T_S[n'(\vec{r})] + \frac{1}{2}\int \frac{[n'(\vec{r})][n'(\vec{r}')]}{|\vec{r} - \vec{r}'|} d\vec{r} d\vec{r}' + E_{xc}[n'(\vec{r})] \tag{3.29}$$

Establishing the Euler-Lagrange equations for a given total number of electron has the form,

$$\delta E_v[n'(\vec{r})] \equiv \int \delta n'(\vec{r}) \left[v_{eff}(\vec{r}) + \frac{\delta}{\delta n'(\vec{r})} T_S[n'(\vec{r})]|_{n'(\vec{r})=n(\vec{r})} - \epsilon \right] d\vec{r} = 0 \tag{3.30}$$

where,

$$v_{eff}(\vec{r}) \equiv v(\vec{r}) + \int \frac{[n(\vec{r}')]}{|\vec{r} - \vec{r}'|} d\vec{r}' + v_{xc}(\vec{r}) \tag{3.31}$$

and,

$$v_{xc}(\vec{r}) \equiv \frac{\delta}{\delta n'(\vec{r})} E_{xc}[n'(\vec{r})]|_{n'(\vec{r})=n(\vec{r})} \tag{3.32}$$

Now, this Euler-Lagrange equation is similar to the form of equation (3.24) for non-interacting particles moving in an effective external potential $v_{eff}(\vec{r})$ on behalf of $v(\vec{r})$. So, the minimizing density can be obtained in a method same as the Hartree approach. The corresponding single-particle Schrödinger equations should represent in the form,

$$\left[-\frac{1}{2}\vec{\nabla}^2 + v_{eff}(\vec{r}) \right] \phi_j(\vec{r}) = \epsilon_j \phi_j(\vec{r}) \qquad j = 1, \ldots, N \tag{3.33}$$

with

$$n(\vec{r}) = \sum_{j=1}^{N} |\phi_j(\vec{r})|^2 \tag{3.34}$$

which construct the self-consistent Kohn-Sham equations.

The ground state energy is denoted as

$$E = \sum_j \epsilon_j + E_{xc}[n(\vec{r})] - \int v_{xc}(\vec{r}) n(\vec{r}) dv - \frac{1}{2} \int \frac{[n(\vec{r})][n(\vec{r}')]}{|\vec{r} - \vec{r}'|} d\vec{r} d\vec{r}' \tag{3.35}$$

If both $E_{xc}[n(\vec{r})]$ and $v_{xc}[n(\vec{r})]$ are neglected together the Kohn-Sham equations lead back to the self-consistent Hartree equations.

The Kohn-Sham equations may be considered as the formal exactification of Hartree approximation which resemble to the Hohenberg-Kohn theorems. The appropriate solution is obtained in case the exact $E_{xc}[n(\vec{r})]$ and $v_{xc}[n(\vec{r})]$ is used.

3.4 Generalized-gradient approximation (GGA)

The generalized-gradient approximation (GGA) for the exchange functional in DFT in connection with correct expressions for the correlation functional

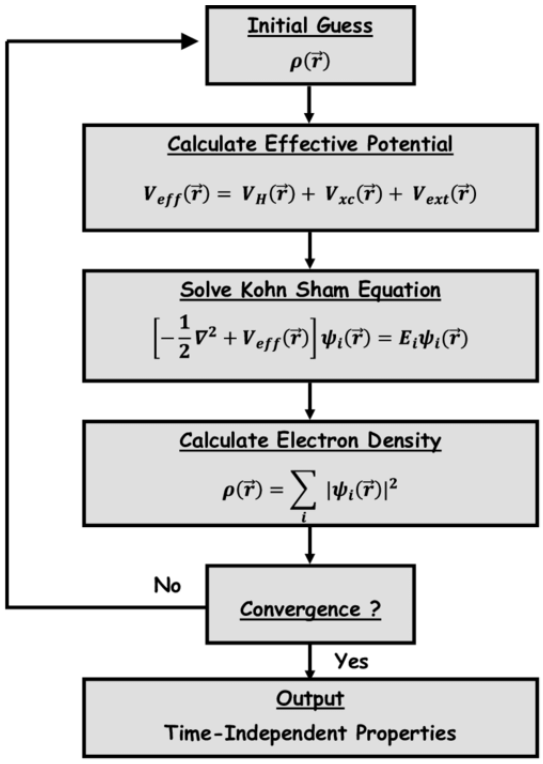

Figure 3.1: Flow chart of a typical time-independent DFT calculation (From Kamal Batra).

have led to enormous applications in which DFT compares quite good with experiment and with the most correct ab initio calculations for properties such as structure, bond energy and reaction activation energies. The GGA explains a variety of processes proposed for functions that modify the behaviour at large gradients in such a process to preserve desired properties. The exchange-correlation energy functional can be expressed as a generalized form of

$$E_{xc}^{GGA}[n^{\uparrow}, n^{\downarrow}] = \int d^3r n(\vec{r}) \epsilon_{xc}(n^{\uparrow}, n^{\downarrow}, |\nabla n^{\uparrow}|, |\nabla n^{\downarrow}|, \ldots) \tag{3.36}$$

$$\equiv \int d^3r n(\vec{r}) \epsilon_x^{hom}(n) F_{xc}(n^{\uparrow}, n^{\downarrow}, |\nabla n^{\uparrow}|, |\nabla n^{\downarrow}|, \ldots) \tag{3.37}$$

It is important to mention that F_{xc} is dimensionless and ϵ_x^{hom} denotes the exchange energy of the unpolarized gas.

For exchange, it is easy to show that there expresses a "spin scaling re-

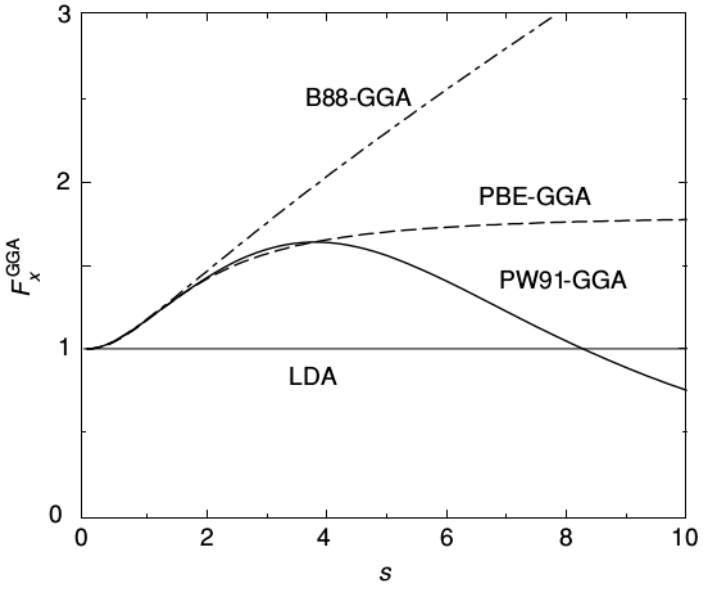

Figure 3.2: Exchange enhancement factor F_x vs the dimensionless density gradient s for various GGAs.

lation",

$$E_x[n^{\uparrow}, n^{\downarrow}] = \frac{1}{2}[E_x[2n^{\uparrow}] + E_x[2n^{\downarrow}]], \tag{3.38}$$

where $E_x[n]$ denotes the exchange energy for an unpolarized system of density $n(\vec{r})$. The spin-unpolarized $F_x(n, |\nabla n|)$ for exchange has taken to consideration. Normally, the dimensionless reduced density gradients of m^{th} order can be represented as

$$s_m = \frac{|\nabla^m n|}{(2k_F)^m n} = \frac{|\nabla^m n|}{2^m(3\pi^2)^{m/3}(n)^{1+m/3}} \tag{3.39}$$

Here, s_m is proportional to the m^{th} order fractional variation in density normalized to the average distance between electrons r_s whereas $k_F = 3(2\pi/3)^{1/3} r_s^{-1}$.

The first gradient can be expressed as

$$s_1 \equiv s = \frac{|\nabla n|}{(2k_F)n} = \frac{|\nabla r_s|}{2(2\pi/3)^{1/3} r_s}. \tag{3.40}$$

The lowest order terms in the expansion of F_x can be computed mathematically,

$$F_x = 1 + \frac{10}{81}s_1^2 + \frac{146}{2025}s_2^2 + \dots \tag{3.41}$$

The factor $F_x(n, s)$ can be explained by the three broadly used forms of Becke (B88), Perdew and Wang (PW91) and Perdew, Burke and Enzerhof (PBE). It is compared for these three approximations in fig (3.2). A better result attained by employing other functionals can be appreciated from the behaviour of these functionals. The GGA is divided into two regions as shown in fig (3.2): (1) small s ($0 < s \lesssim 3$) and (2) large s ($s \gtrsim 3$).

In region (1), small s is suitable for most physical applications, different $F_x s$ have nearly uniform shapes, which is the reason that different GGAs provide homogeneous improvement for many conventional systems with small density gradient contributions. GGAs give an exchange energy lower than the LDA for $F_x \geq 1$. Generally, there are more swiftly varying density regions in atoms than in condensed matter, which provides greater reduction of the exchange energy in atoms than in molecules and solids. The most significant features of present GGAs is the results in the lowering of binding energy, correcting the LDA overbinding and progressing agreement with experiment. The average value of the increment is roughly 4/3, generating the average exchange resembles to that proposed by Slater in the range $0 < s \lesssim 3$, although for very different reasons. By the use of this factor 4/3 or an adjustable factor called "$X\alpha$" that tends to be between 1 and 4/3 for this improvement.

In region (2), because of choosing different physical conditions for $s \to \infty$, $F_x s$ generates the different limiting behaviours. In B88-GGA, $F_x^{B88-GGA}(s) \sim s/ln(s)$ was chosen to provide the accurate exchange energy density ($\epsilon_x \to -1/2r$). In PW91-GGA, $F_x^{PW91-GGA}(s) \sim 1/\sqrt{s}$ was chosen to satisfy the Lieb-Oxford bound and the non-uniform scaling condition that have to be satisfied in case the functional is to have the proper limit for a thin layer

or a line. In PBE-GGA, $F_x^{PBE-GGA}(s) \sim const$ was chosen to drop the non-uniform scaling condition in favor of a simplified parameterization. Because of choosing different physical conditions, $F_x s$ generates the different behaviour in region (2) not only views the lack of knowledge of the large density gradient regions but also an inherent difficulty of the density gradient expansion in this region, even if one form of GGA somehow provides the qualitative result for a certain physical property while others fail, it is not expected that the form is preferred for other properties in which different physical condition exist.

3.5 Explicit PBE form

The PBE form is one kind of exchange-correlation functional of GGA functional. It is likely the simplest GGA functional. The PBE functional for exchange is provided by a simple form for the expansion factor F_x. The form is explained with $F_x(0) = 1$ and $F_x \to constant$ at large s,

$$F_x(s) = 1 + \kappa - \kappa/(1 + \mu s^2/\kappa) \tag{3.42}$$

It is important to mention that the value of $\kappa = 0.804$ is chosen to fulfill the Lieb-Oxford bound. $\mu = 0.21951$ is chosen to restore the linear response form of the local approximation, i.e. it is chosen to avoid the term from the correlation.

The form for correlation is introduced as the local correlation plus an additive term both of this depend upon the gradients and the spin polarization. The form chosen to fulfill some condition is

$$E_c^{GGA-PBE}[n^{\uparrow}, n^{\downarrow}] = \int d^3 r n[\epsilon_c^{hom}(r_s, \zeta) + H(r_s, \zeta, t)] \tag{3.43}$$

where, $\zeta = (n^{\uparrow}, n^{\downarrow})/n$ denotes the spin polarization, r_s denotes the local value of the density parameter and t represents a dimensionless gradient

$t = |\nabla n|/2\phi k_{TF} n$. Here, $\phi = ((1+\zeta)^{2/3} + (1-\zeta)^{2/3})$ and t can be scaled by the screening wave factor k_{TF} rather than k_F. The Final form can be written as

$$H = \frac{e^2}{a_0}\gamma\phi^3 \log\left(1 + \frac{\beta}{\gamma}t^2 \frac{1 + At^2}{1 + A^2 + A^2t^4}\right) \tag{3.44}$$

where, a_0 represents Bohr radius and the factor e^2/a_0 is unity in atomic unit. The function A is expressed as

$$A = \frac{\beta}{\gamma}\left[\exp\left(\frac{-\epsilon_c^{hom}}{\gamma\phi^3 \frac{e^2}{a_0}}\right) - 1\right]^{-1} \tag{3.45}$$

Chapter 4

Results and discussion

4.1 Methodology

The size of the basis set in these calculations was controlled by the parameter $R_{\mathrm{Kmax}} = R_{\mathrm{mt}} \times K_{\mathrm{max}}$ which was chosen 6 (R_{mt} and K_{max} indicates the smallest muffin tin radius and the largest wave number of the basis set respectively) and the initial Brillouin zone integration in the k-space was done by 1000 k-points for each unit cell. During the self-consistent process, the energy, charge, and force thresholds were set to 10^4 eV, 10^3 electrons per atom, and 10^3 Ry/a.u., respectively. The graphite crystalline structure was initially considered when simulating the graphene layer. The interlayer

Spacegroup	P6/mmm
a	$2.45\mathring{A}$
b	$2.45\mathring{A}$
c	$15\mathring{A}$
α	90°
β	90°
γ	120°

Table 4.1: Parameter used in SCF calculation.

spacing was then increased until the energy changes converted to the nec-

essary value (less than 0.001 eV) to avoid interaction between two carbon layers in the graphite structure. To simulate pure and impure graphene, the supercell approach was applied. The influence of Fe impurities and vacancies on graphene characteristics was investigated using many $3 \times 3 \times 1$ supercells with various defect positions and concentrations. To achieve FM graphene, certain C atoms were replaced with Fe atoms or removed at the same sublattices to meet these requirements.

4.2 Electronic properties

Primitive graphene exhibits zero band gap with linear dispersion relation around the E_F but the electronic properties of doped graphene and vacant graphene are modified, notably the electronic DOS. The value of E_g is proportional to the doping concentration of any types of adatoms. But it is effective to a certain number of doping concentration. Upto this certain number of doping concentration, the value of E_g does not depend on the doping type. Furthermore, one can also deduce that the value of E_g rises almost linearly with any type of doping concentration. The modification of TDOS due to doping of Fe and vacancy of its own atom has been depicted in fig-(4.1), (4.2) and (4.3) . Fig-(4.1), (4.2) and (4.3) represent the primitive structure along with its TDOS.

In fig-(4.1), (4.2) and (4.3), B, C and D represent the doped, vacancy and both doped and vacancy system respectively. To define the contribution of each atomic orbital in chemical bonding, the partial density of state (PDOS) for both C 2s and 2p and Fe 3d orbitals are deliberated. The 3d orbital of the iron atom is deffused in the energy limit resembling to the 2s and 2p orbitals of their nearby neighbor carbon atoms. To maintain metallic behavior, the sp^2 bands of graphene hybridize with the 3d orbital of iron and creates strong covalent bond between them at Fermi energy.

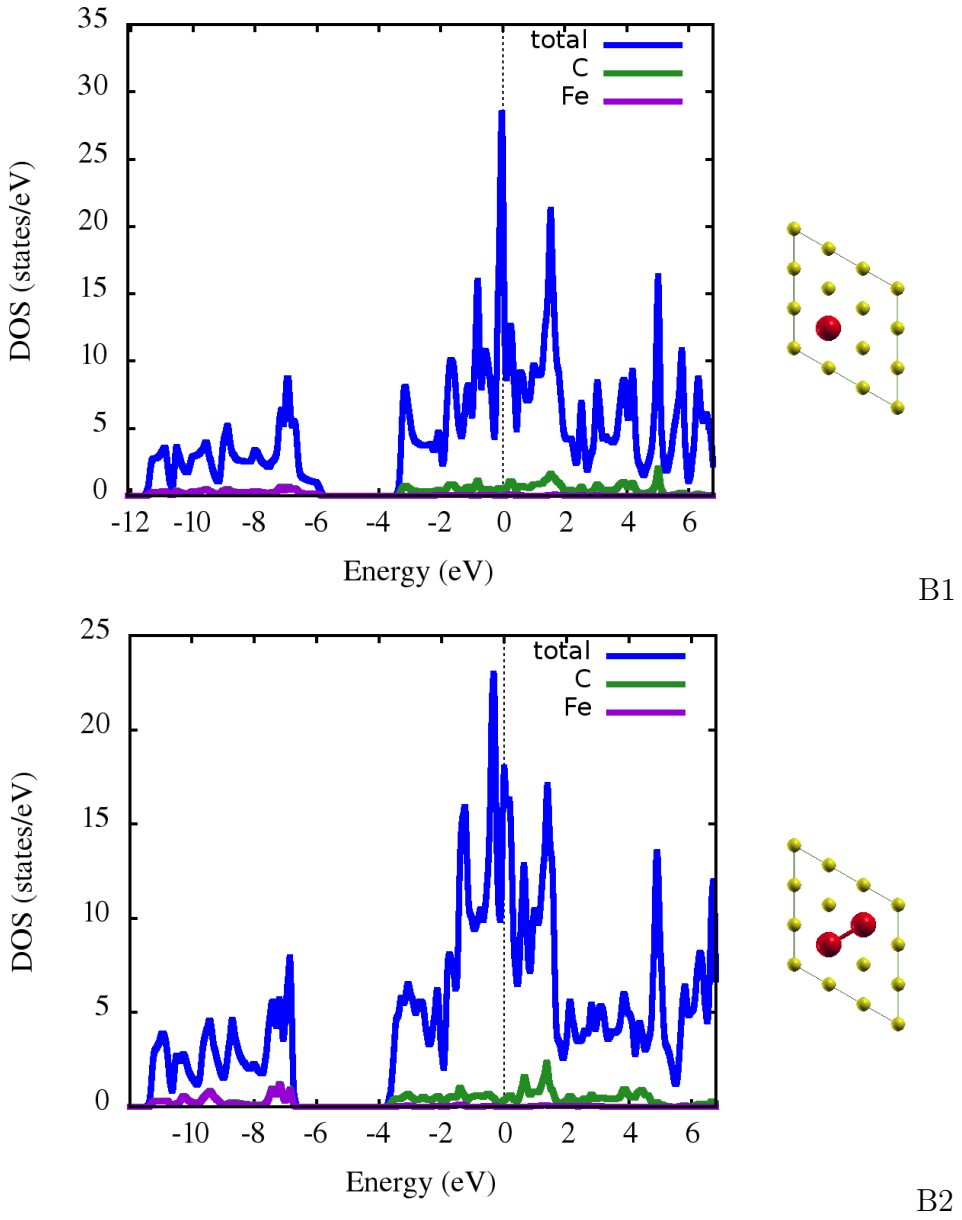

Figure 4.1: The TDOS and structure of the supercells (Fe doped).

4.3 Magnetic properties

The exchange interactions between magnetic impurities embedded in graphene are mediated by conduction electrons of the host. To explain the indirect exchange interaction for metal's intrinsic magnetic form, the RKKY (Ruderman-Kittle-Kasuya-Yosida) theory is the efficient model. The RKKY theory is also applicable for highly degenerate semiconductors. Various type of studies remain for the RKKY coupling in graphene, where the standard perturbative approach applied to a continuum field-theoretic description of

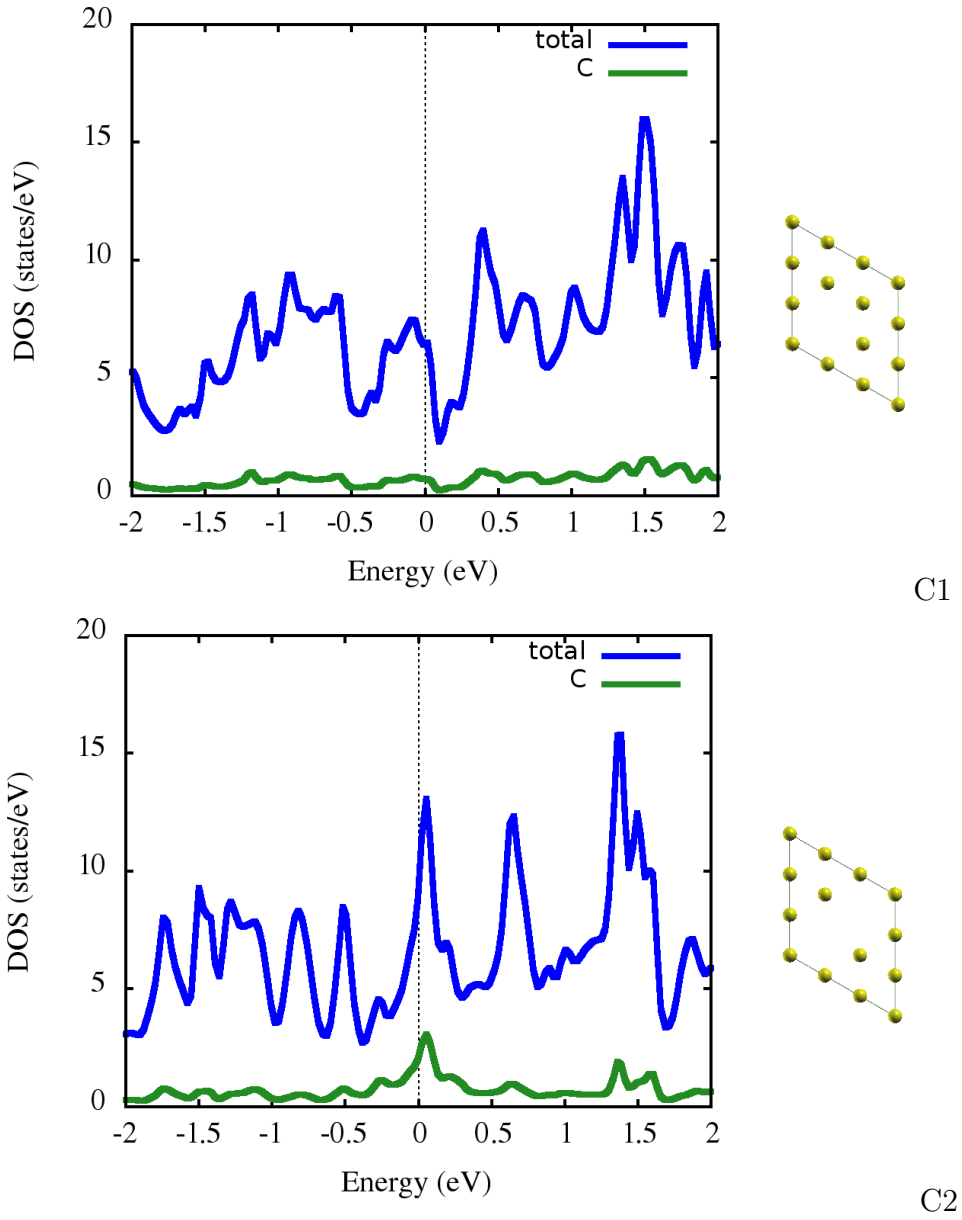

Figure 4.2: The TDOS and structure of the supercells (atom vacancy).

graphene and exact diagonalization on a finite size lattice have similar results.

The origin of the RKKY exchange interactions are observed by the PDOS of the C and Fe atoms. The magnetic properties of graphene supercells indicate due to the hybridizations between 3d orbital of iron atoms and 2s and 2p orbitals of carbon atoms. The magnetic moment of these graphene supercells are given in table 4.2. The magnetic moment of a free Fe is 2.22

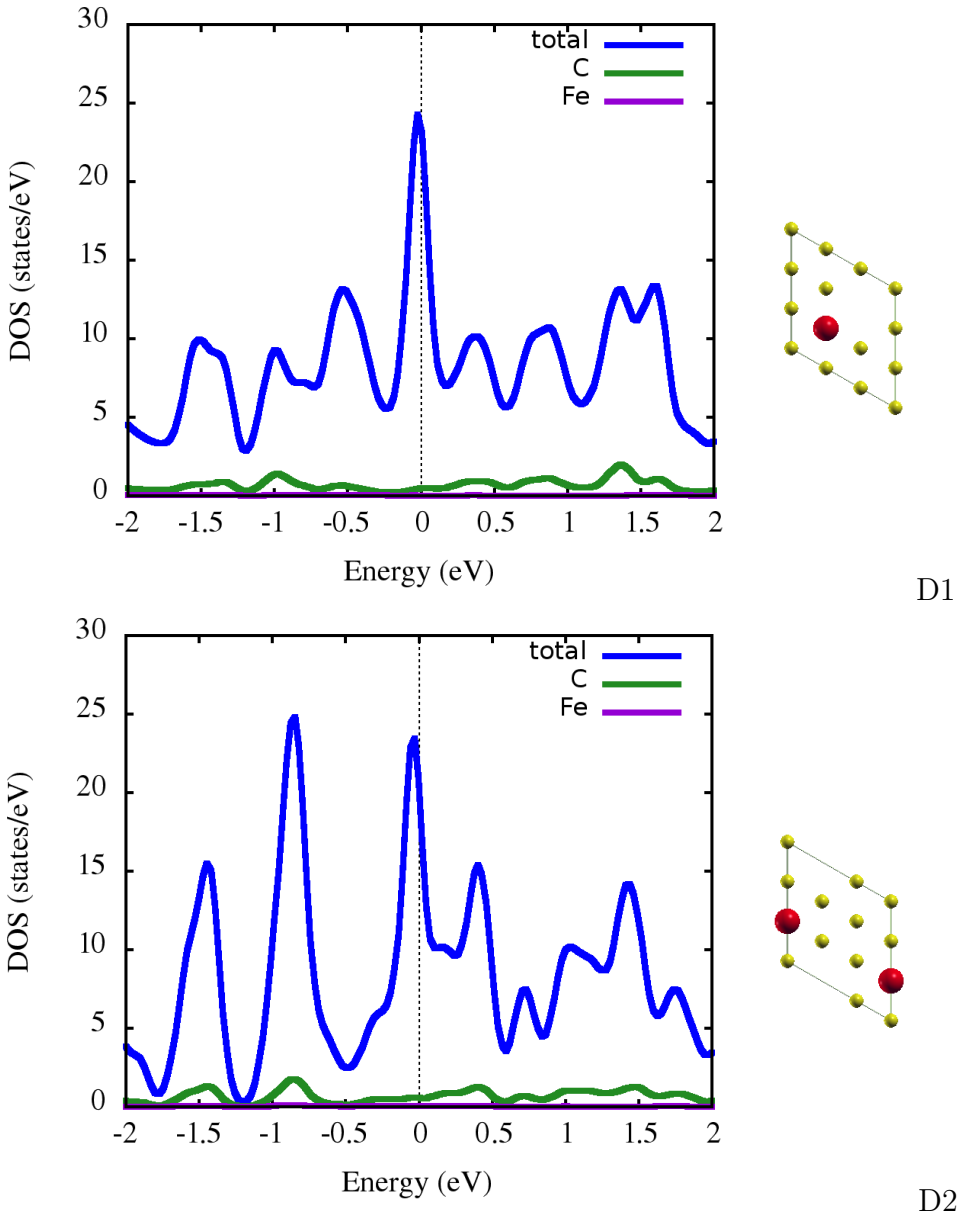

Figure 4.3: The TDOS and structure of the supercells (both Fe doped and atom vacancy).

μB. But when Fe atom is embedded in graphene, the magnetic moment is decreased to 1.3496. The minimize of electrons with majority spins in Fe atom by hybridization between their 3d orbitals and sp^2 orbitals of C atoms is the main reason for this decrement. One Fe atom in graphene structure doesn't have the monotonic effect on the magnitude of the magnetic moment. But the increase of the concentration of Fe atom in the graphene structure rises the magnetic moment. The distance between Fe atoms in the supercells also transforms this magnitude. The magnetic moment is lower

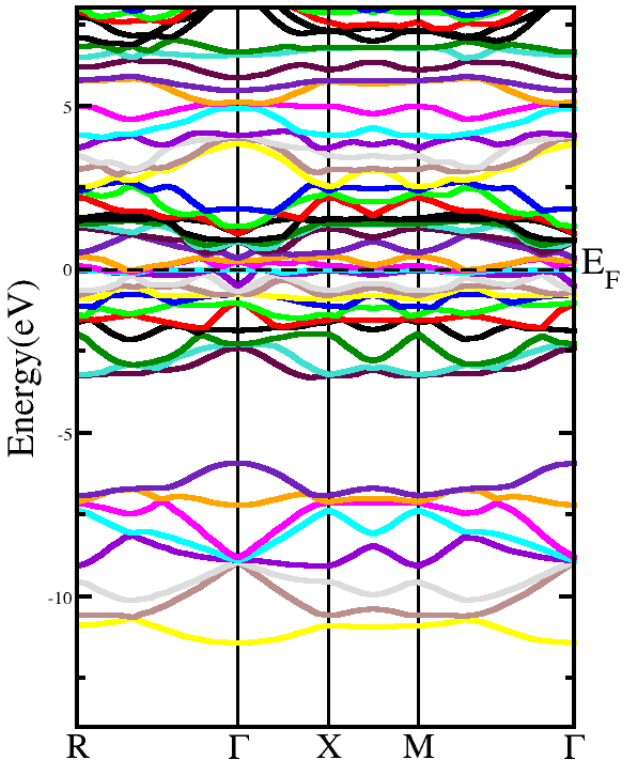

B1

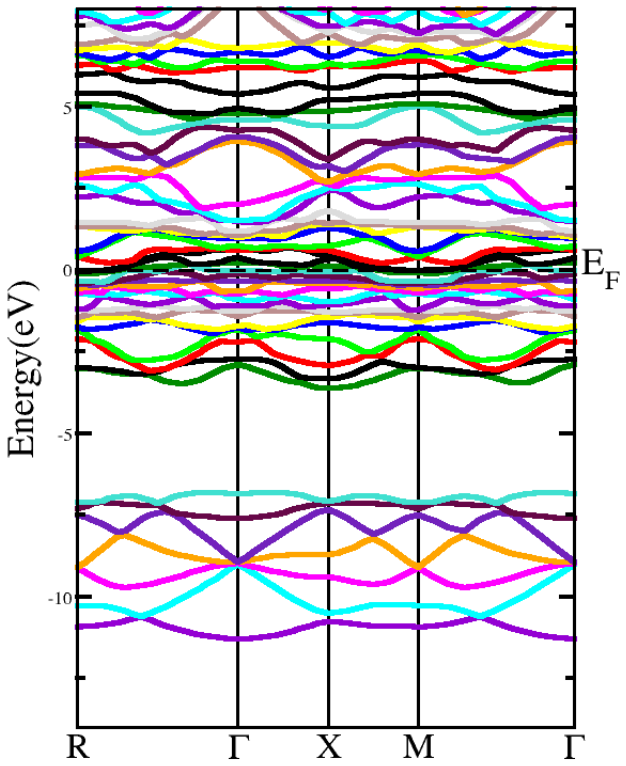

B2

Figure 4.4: Band structure of the supercells (Fe doped).

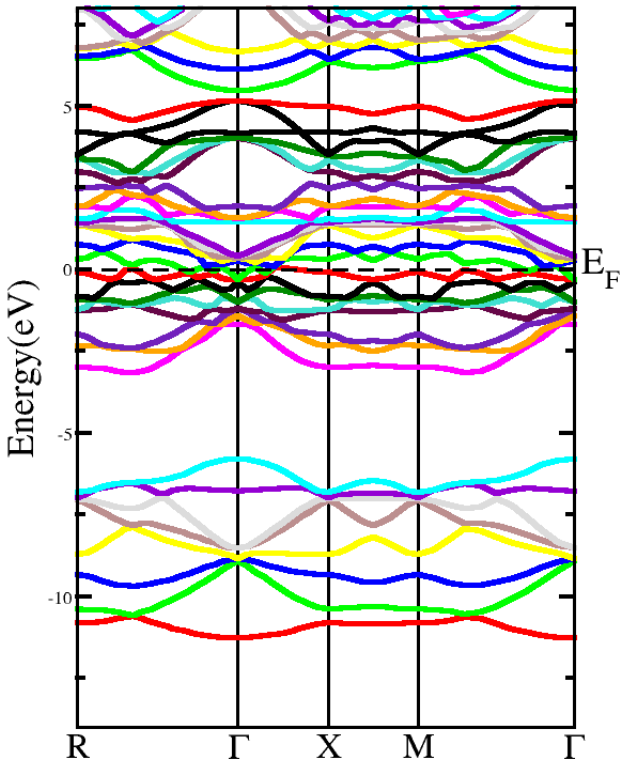

C1

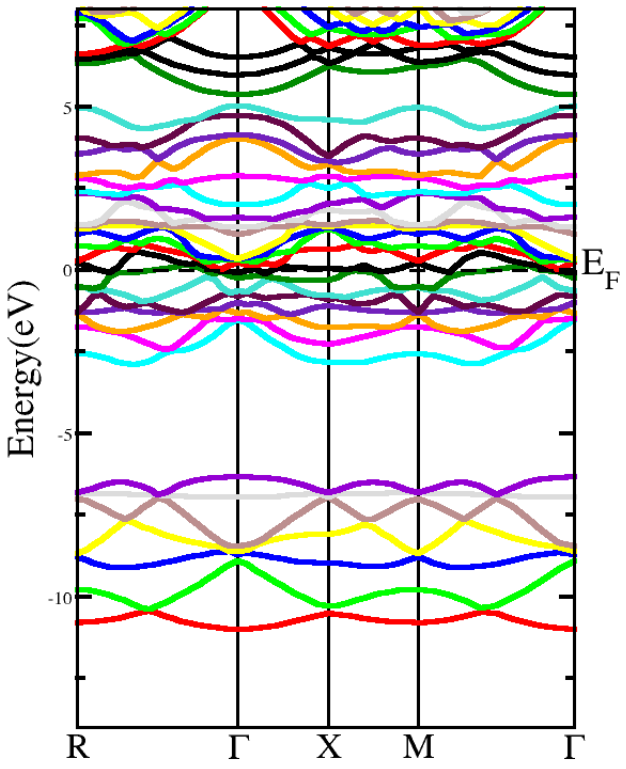

C2

Figure 4.5: Band structure of the supercells (atom vacancy).

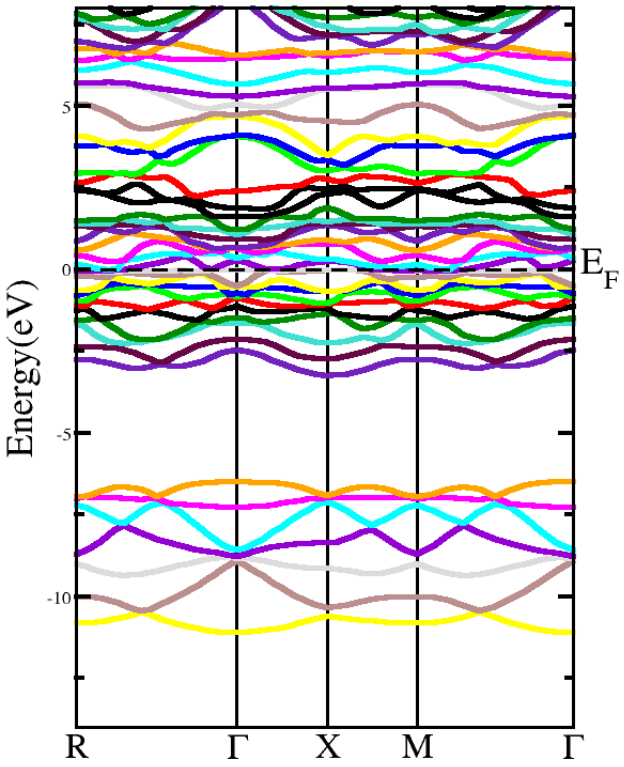

D1

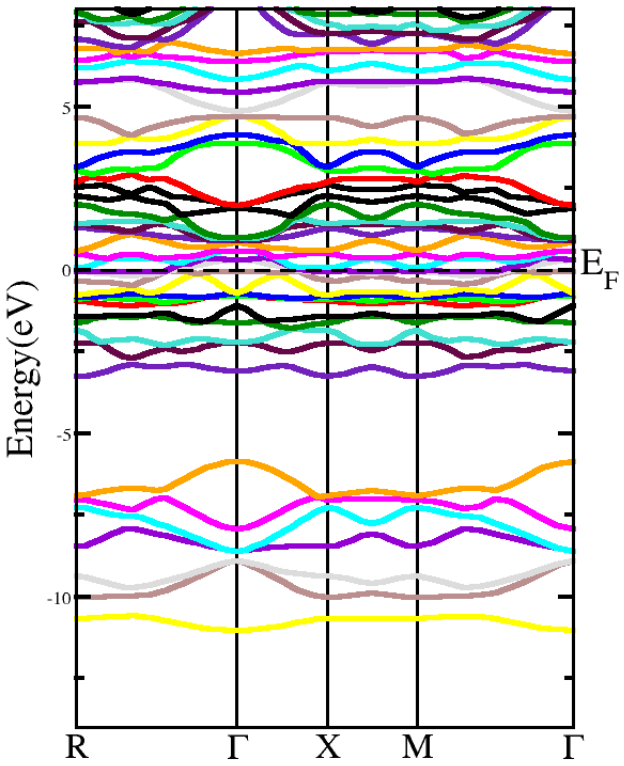

D2

Figure 4.6: Band structure of the supercells (both Fe doped and atom vacancy).

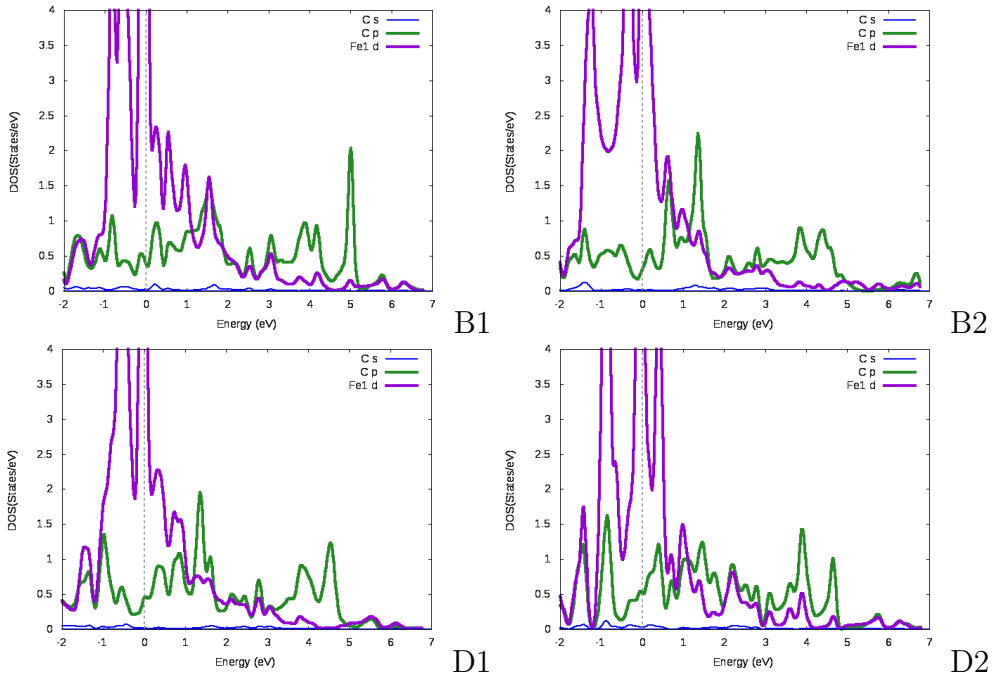

Figure 4.7: The PDOS of the supercells.

No.	Total Energy (Ry)	Magnetic Moment (μB/cell)
B_1	-3151.87550948	1.34963
B_2	-5621.61120669	5.26898
C_1	-606.26886482	0.91835
C_2	-530.41816819	1.45915

Table 4.2: The energy difference and magnetic moment of the supercells.

due to the higher separation between Fe atoms because the indirect exchange interactions are dependent on the distance between magnetic atoms.

Another process to generate magnetic influence is the vacancy created in the graphene structure. When a C atom remove from the graphene structure, one sp^2 dangling bond will obtain. This dangling bond is generated by the three nearest neighbor atoms around the vacancy and two of them share their electrons and construct the pentagon on behalf of the hexagon. Magnetic moment is attained by this third unsaturated bond. Hence, the vacancies behave as embedded magnetic atoms in graphene structure. But the obtained magnetic moment due to generate vacancies is lower than the magnetic moment in presence of Fe impurities. The difference in the efficient

number of unpaired spins of them is the main reason for that. The increase of the concentration of vacancies and distance between vacancies transform this magnitude of magnetic moment but it is not so high. Detailed discussion of experimental and theoretical studies in presence of vacancies.

4.4 Optical properties

In this section, dielectric function, absorption spectra, electron energy loss spectra (EELS), reflectivity and refractive index are included.

4.4.1 Dielectric function

In fig-(4.8), the real and imaginary parts of the dielectric function versus the photon energy of electric field of electromagnetic wave to graphene plane change at different frequencies relative to the primitive graphene. The magnitudes of real and imaginary parts of the dielectric function decrease roughly beyond 1.5 ev in fig-(4.8).

The value of static dielectric constant (Re $\epsilon(0)$) for primitive graphene is 2.4 corresponding to the computation done by Palash Nath et al. By virtue of embedding defects, this quantity increases strongly. But the increase of the defect concentration falls the static dielectric constant for the conversion to the case of magnetic moment. Usually replacing the C atoms with Fe impurities has more impact on static dielectric constant relative to the vacancies of C atom.

The imaginary part of the dielectric function stay identical like real part. The maximum peak of Im $\epsilon(\omega)$ finds in the visible region of pure graphene. But the quantity turns to the infrared(IR) region for defected graphene. This is the outcomes of closely separated flat electronic bands around the Fermi level. The concentration of defects and distance between them in

each supercell are main reason for this turn.

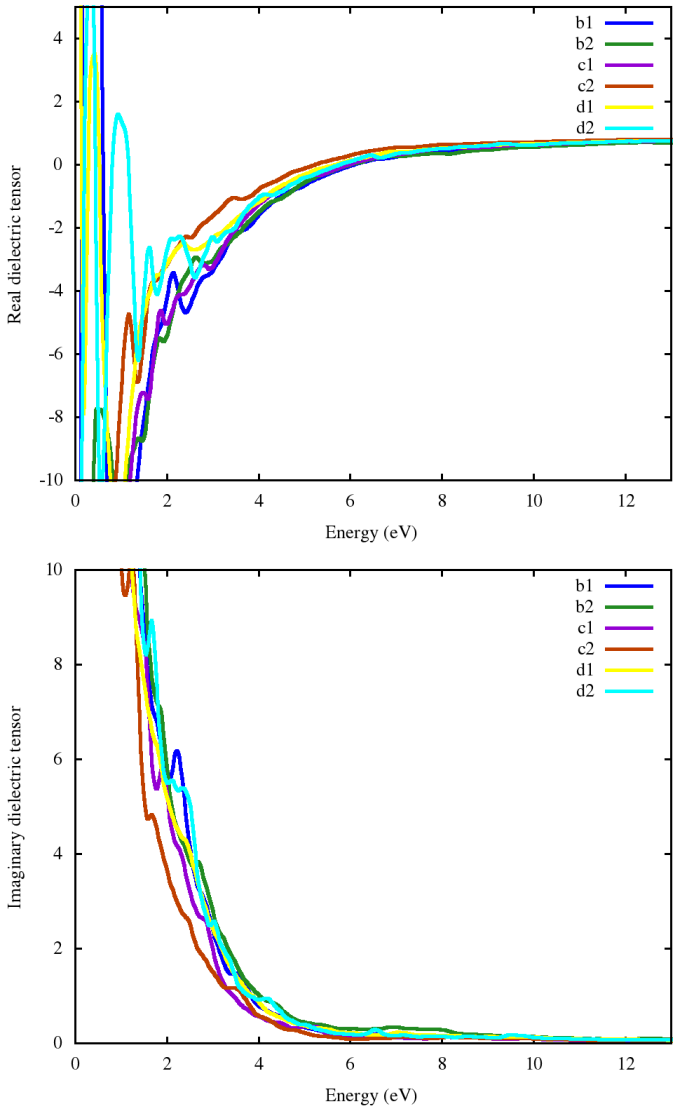

Figure 4.8: The real and imaginary part of the dielectric function for the supercells.

4.4.2 Absorption spectra and Electron energy loss spectra (EELS)

In Fig-(4.9), the optical absorption spectra for parallel polarization of an electromagnetic wave's electric field for both pure and defective graphene are displayed.Pure graphene has a maximum peak about 2.7 eV, which corresponds to the imaginary part of the dielectric function's maximum peak.

Because of the increase in the number of free carriers, inserting flaws in the graphene structure causes the optical absorption spectra to broaden in the visible to IR region. To put it another way, some peaks near the Fermi level in the DOS plot indicate the presence of extra carriers in the low energy level, which leads to the inter band transition and hence adsorption in the low frequency photon.

In addition, the JDOS curves show some peaks at low energies, showing that photon absorption occurs in this range. Changes in concentration and distance between defects have less impact on the absorption curve. Fig-(4.9) shows the EELS for different considered cases and electric field parallel illumination. At low energies, these spectra show EELS decrease. For pure graphene, there are two peaks around 4 eV and 4.4 eV with 1.84 and 1.75 intensities respectively that are related to in plane Plasmon excitations. The resulting results are consistent with the experimental data available. The presence of impurities in the graphene structure causes the EELS peaks to have a larger amplitude and energy. However, when the quantity of contaminants rises, the amplitude of EELS peaks decreases, becoming broader and shorter. In optical gas sensors that detect changes in electronic characteristics, lowering the EELS intensity is beneficial. The amplitude of EELS diminishes in the energy range associated to the greatest absorption peaks, as shown in Fig-(4.9). As a result, these structures are appropriate for optical gas sensing, which detects variations in photo-current caused by gas absorption.

4.4.3 Reflectivity and Refractive index

Fig-(4.10) shows the real component of the refractive index (N) and reflectivity vs incident photon energy for parallel polarization of an electromagnetic wave's electric field. According to this diagram, the maximum refractive index for pure graphene is around 2.18 in the visible area, but in the event of defected graphene, this quantity rapidly increases and shifts to the IR

region. In reality, the size and energy of the maximum refractive index are affected by the concentration, nature, and distance between defects. The magnitude of the maximum refractive index in the presence of Fe impurities, for example, is greater than in the absence of vacancies. However, as seen in fig-(4.10), this quantity decreases as the impurity concentration rises and the distance between impurity sites decreases.

It should be noted that the refractive index of the system is directly proportional to its magnetic moment (μ), as shown by the relationship $N = \sqrt{\mu\epsilon}$, which demonstrates the relationship between refractive index and magnetic characteristics. As a result, changing the magnetic moment allows for refractive index engineering. The refractive index can be used to calculate the reflectivity of pure and impure graphene structures for parallel polarization of the electric field. Pure graphene has a maximum reflectivity of 3.2 eV, which corresponds to a magnitude of 0.27. Zero or very tiny reflectivity is found in the energy range greater than 6 eV, which is connected to the modest values of two portions of the dielectric function at this range. The reflectivity spectra of impure graphene differ greatly from those of pure graphene. Reflectivity is low in the visible and infrared ranges for pure graphene, and it is zero at higher energies. The degree of reflectance in the IR to ultra violet (UV) band increases when C atoms are replaced with vacancies or Fe atoms. The increase in free carrier density causes the rise in reflectance. Absorption and reflection become modest for energy ranges greater than 6 eV. As a result, defected graphene behaves similarly to pure graphene in this range, and both are transparent in the deep ultraviolet.

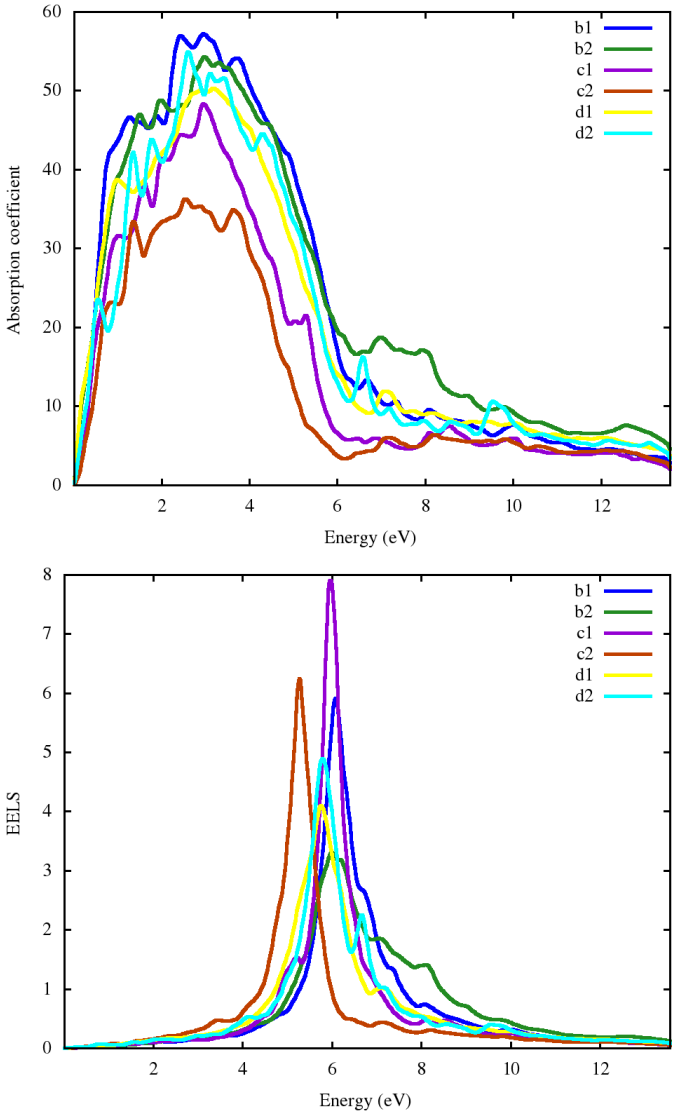

Figure 4.9: The absorption coefficient and EELS for the supercells.

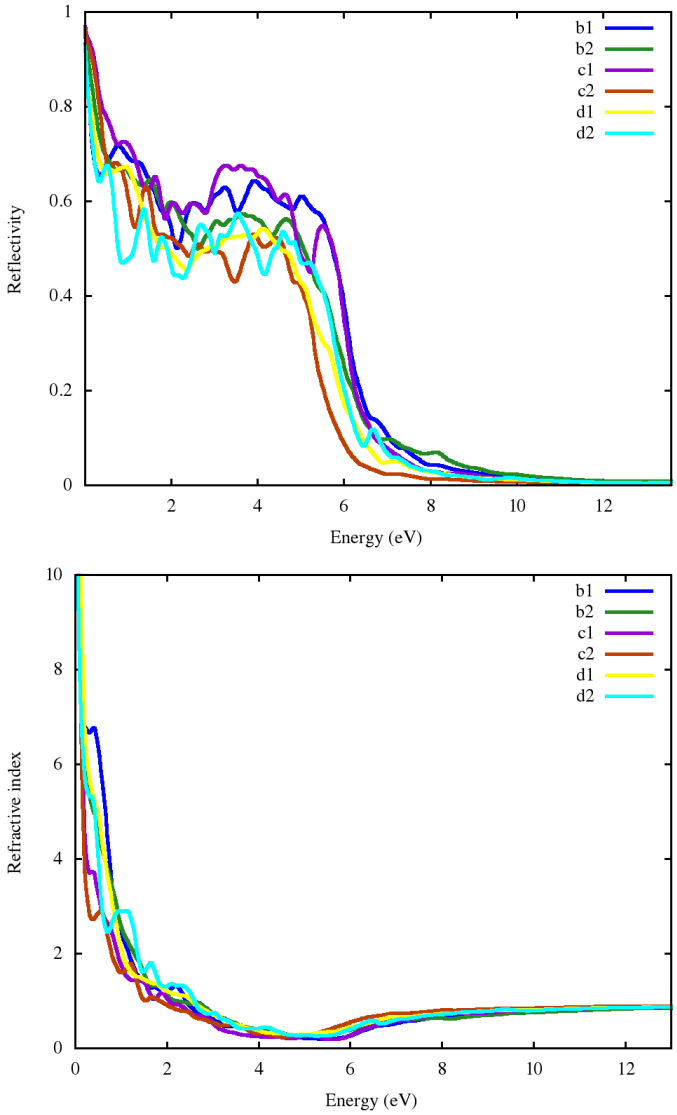

Figure 4.10: The Reflectivity and refractive index for the supercells.

Chapter 5

Conclusions

It is demonstrated through the DFT calculation within GGA that doping of Fe and vacancies at graphene structure conspicuously alter the magnetic and optical properties of graphene. It has been shown that the presence of Fe impurities and vacancies at graphene structure can not change the electronic property of graphene that means the conductive behaviour of graphene remains. According to the obtained results, the FM phase is the most feasible point by substituting the Fe atoms and vacancies in the sublattice of graphene. Besides, the magnetic moment of supercells increases due to increasing the vacancy and Fe atom concentrations as well as reduces by increasing the distance between Fe atoms. It occurs because the distance between magnetic atoms is dependent on the indirect exchange interactions. But the distance between vacancies can't have any significant effect on the magnetic moment of supercells.

On the whole, substituting Fe for C atoms has a greater impact on magnetic and optical properties than C vacancies.

Appendix A

List of Abbreviations

BZ	:	Brillouin Zone
DFT	:	Density Functional Theory
DOS	:	Density of States
GGA	:	Generalized Gradient Approximation
HK	:	Hohenberg-Kohn
KS	:	Kohn-Sham
LSDA	:	Local Spin Density Approximation
SOC	:	Spin Orbit Coupling
XC	:	Exchange correlation

Bibliography

[1] A. Szabo and N.S. Ostlund. Modern Quantum Chemistry. McGraw-Hill, 1989.

[2] W. Kohn. Nobel lecture: Electronic structure of matter - wave functions and density functionals. Reviews of Modern Physics, 71:1253-1266, 1999.

[3] W. Kohn and L.J. Sham. Self-consistent equations include exchange and correlation effects. Physical Review, 140:A1133-A1138, 1965.

[4] Erwin Schrödinger An undulatory theory of the mechanics of atoms and molecules. Physical Review, 28:1049-1070, 1926.

[5] F. Schwabl. Quantenmechanik: Eine Einführung (German) . Springer, 2007.

[6] M. Born. On the quantum mechanics of collision processes (german). Zeitschrift fuer Physik, 37:863-867, 1926.

[7] W. Koch and M.C. Holthausen. A Chemists's Guide to Density Functional Theory. Wiley-VCH, 2001.

[8] W. Pauli. The connection between spin and statistics. Phys. Rev., 58:716-722, 1940.

[9] N. Zettili. Quantum Mechanics: Concepts and Applications. Wiley-VCH, 2009.

[10] K. Capelle. A bird's-eye view of density-functional theory. arXiv:cond-mat, 0211443v5, 2006.

[11] D.A. McQuarrie and J.D. Simon. Physical Chemistry: A Molecular Approach . University Sciency Books, 1997.

[12] W. Koch and M.C. Holthausen. A Chemists's Guide to Density Functional Theory. Wiley-VCH, 2001.

[13] M. Levy and A. Nagy. Variational density-functional theory for an individual excited state. Phys. Rev. Lett., 83:4361pp, 1999.

[14] T. Flieÿbach. Mechanik: Lehrbuch zur Theoretischen Physik I (German). Spektrum, 2009.

[15] A. Berger. Current-Density Functional in Extended Systems. PhD thesis, Rijksuni-versiteit Groningen, 2006.

[16] P. Hohenberg and W. Kohn. Inhomogeneous electron gas. Physical Review, 136:B864-B871, 1964.